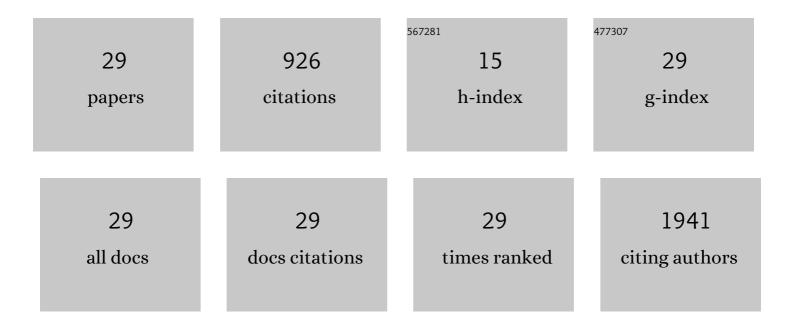
Patrick W Hales

List of Publications by Year in descending order

Source: https://exaly.com/author-pdf/4439706/publications.pdf Version: 2024-02-01



DATRICK W/ HALES

#	Article	IF	CITATIONS
1	Highâ€resolution microscopic diffusion anisotropy imaging in the human hippocampus at 3T. Magnetic Resonance in Medicine, 2022, 87, 1903-1913.	3.0	4
2	Venous cerebral blood flow quantification and cognition in patients with sickle cell anemia. Journal of Cerebral Blood Flow and Metabolism, 2022, , 0271678X2110723.	4.3	8
3	Individual Watershed Areas in Sickle Cell Anemia: An Arterial Spin Labeling Study. Frontiers in Physiology, 2022, 13, 865391.	2.8	8
4	Comparison of models of diffusion in Wilms' tumours and normal contralateral renal tissue. Magnetic Resonance Materials in Physics, Biology, and Medicine, 2021, 34, 261-271.	2.0	2
5	Tractographic and Microstructural Analysis of the Dentato-Rubro-Thalamo-Cortical Tracts in Children Using Diffusion MRI. Cerebral Cortex, 2021, 31, 2595-2609.	2.9	13
6	Comparison Between Diffusionâ€Weighted MRI and ¹²³ lâ€mIBG Uptake in Primary Highâ€Risk Neuroblastoma. Journal of Magnetic Resonance Imaging, 2021, 53, 1486-1497.	3.4	7
7	Classification of paediatric brain tumours by diffusion weighted imaging and machine learning. Scientific Reports, 2021, 11, 2987.	3.3	25
8	Neurosurgical applications of tractography in the UK. British Journal of Neurosurgery, 2021, 35, 424-429.	0.8	7
9	Quantitative MRI demonstrates abnormalities of the third ventricle subventricular zone in neurofibromatosis type-1 and sporadic paediatric optic pathway glioma. NeuroImage: Clinical, 2020, 28, 102447.	2.7	2
10	Combined Denoising and Suppression of Transient Artifacts in Arterial Spin Labeling <scp>MRI</scp> Using Deep Learning. Journal of Magnetic Resonance Imaging, 2020, 52, 1413-1426.	3.4	15
11	Vascular Instability and Neurological Morbidity in Sickle Cell Disease: An Integrative Framework. Frontiers in Neurology, 2019, 10, 871.	2.4	30
12	Arterial spin labelling and diffusion-weighted imaging in paediatric brain tumours. Neurolmage: Clinical, 2019, 22, 101696.	2.7	31
13	An alternative approach to contrast-enhanced imaging: diffusion-weighted imaging and T1-weighted imaging identifies and quantifies necrosis in Wilms tumour. European Radiology, 2019, 29, 4141-4149.	4.5	7
14	The promise of noninvasive cerebral hemodynamic assessment in sickle cell anemia. Neurology, 2018, 90, 585-586.	1.1	3
15	Cerebral perfusion characteristics show differences in younger versus older children with sickle cell anaemia: Results from a multipleâ€inflowâ€time arterial spin labelling study. NMR in Biomedicine, 2018, 31, e3915.	2.8	13
16	Volumetric assessment of tumor size changes in pediatric low-grade gliomas: feasibility and comparison with linear measurements. Neuroradiology, 2018, 60, 427-436.	2.2	22
17	Delineation of the visual pathway in paediatric optic pathway glioma patients using probabilistic tractography, and correlations with visual acuity. NeuroImage: Clinical, 2018, 17, 541-548.	2.7	22
18	Quantitative MRI in post-operative paediatric cerebellar mutism syndrome. European Journal of Radiology, 2018, 108, 43-51.	2.6	14

PATRICK W HALES

#	Article	IF	CITATIONS
19	A general model to calculate the spin-lattice (T ₁) relaxation time of blood, accounting for haematocrit, oxygen saturation and magnetic field strength. Journal of Cerebral Blood Flow and Metabolism, 2016, 36, 370-374.	4.3	45
20	Multi entre reproducibility of diffusion MRI parameters for clinical sequences in the brain. NMR in Biomedicine, 2015, 28, 468-485.	2.8	178
21	A multiâ€Gaussian model for apparent diffusion coefficient histogram analysis of Wilms' tumour subtype and response to chemotherapy. NMR in Biomedicine, 2015, 28, 948-957.	2.8	34
22	Arterial Spin Labeling Characterization of Cerebral Perfusion during Normal Maturation from Late Childhood into Adulthood: Normal †Reference Range' Values and Their Use in Clinical Studies. Journal of Cerebral Blood Flow and Metabolism, 2014, 34, 776-784.	4.3	61
23	Interrogation of living myocardium in multiple static deformation states with diffusion tensor and diffusion spectrum imaging. Progress in Biophysics and Molecular Biology, 2014, 115, 213-225.	2.9	19
24	Comparison of ASL and DCE MRI for the non-invasive measurement of renal blood flow: quantification and reproducibility. European Radiology, 2014, 24, 1300-1308.	4.5	50
25	Combined Arterial Spin Labeling and Diffusion-Weighted Imaging for Noninvasive Estimation of Capillary Volume Fraction and Permeability-Surface Product in the Human Brain. Journal of Cerebral Blood Flow and Metabolism, 2013, 33, 67-75.	4.3	33
26	A Two-Stage Model for In Vivo Assessment of Brain Tumor Perfusion and Abnormal Vascular Structure Using Arterial Spin Labeling. PLoS ONE, 2013, 8, e75717.	2.5	11
27	Histo-anatomical structure of the living isolated rat heart in two contraction states assessed by diffusion tensor MRI. Progress in Biophysics and Molecular Biology, 2012, 110, 319-330.	2.9	96
28	Progressive changes in <i>T</i> ₁ , <i>T</i> ₂ and leftâ€ventricular histoâ€architecture in the fixed and embedded rat heart. NMR in Biomedicine, 2011, 24, 836-843.	2.8	31
29	Generation of histo-anatomically representative models of the individual heart: tools and application. Philosophical Transactions Series A, Mathematical, Physical, and Engineering Sciences, 2009, 367, 2257-2292.	3.4	135